

In situ electrochemical organization of CdSe nanoclusters on graphene during unzipping of carbon nanotubes†

Joyashish Debgupta, Dhanraj B. Shinde and Vijayamohan K. Pillai*‡

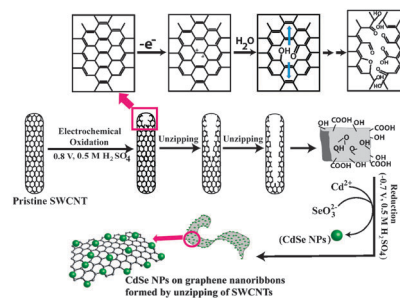
Received 11th December 2011, Accepted 30th January 2012

DOI: 10.1039/c2cc17749h

In situ decoration of very small CdSe quantum dots on graphene nanoribbons (GNRs) has been achieved during the electrochemical unzipping of single walled carbon nanotubes. Critical parameters like the width of the GNRs, size distribution of quantum dots and their organization on GNRs have been shown to be strongly dependent on the electric field and time.

Graphene is a one-atom thick, two-dimensional sheet of carbon atoms considered as the mother of all types of graphitic carbon allotropes which exhibits many exciting properties, like long-range ballistic transport,¹ due to the availability of carriers such as Dirac fermions.² On the other hand, CdSe nanoparticles are well-known for their size as well as shape-dependent optical behavior originating from the effect of quantum confinement of electrons in these quantum dots.³ Combining these two nanomaterials could produce interesting hybrids having excellent yet tunable optical, photo-catalytic, optoelectronic properties⁴ enabling their use in solar cells, flexible optoelectronic materials, sensors, biological imaging *etc.* Despite the unique opportunities in terms of novel properties expected by modulating the width of graphene nanoribbons, studies on graphene–CdSe composites are only very few.

Almost all the synthetic methods involve indirect chemical methods⁵ and to the best of our knowledge there is no report on the *in situ* formation of CdSe nanoclusters on graphene and that too by any electrochemical approach. The closest report describes the importance of silica template-assisted growth of aligned CdSe nanodots through electrodeposition.⁶ However, no report has focused on the quality or source of graphene and almost all of the available reports use graphene chemically prepared from graphite. Recent methods of preparation of graphene by the longitudinal unzipping of carbon nanotubes (by using laser irradiation or electric field) are interesting due to their topological connection with carbon nanotubes since carbon nanotubes could be considered as seamlessly rolled sheets of graphene.⁷ A related electrochemical unzipping of



Scheme 1 Electrochemical unzipping of SWCNTs and subsequent CdSe nanoparticle decoration on the *in situ* formed GNRs.

CNTs to form high quality graphene nanoribbons has been reported very recently by our group.⁸ More significantly, this electrochemically prepared graphene nanoribbon is of superior quality in terms of less defect contents and ease of fabrication. Consequently, the possibility of heterojunction formation using monodispersed CdSe NPs might be interesting due to unique properties imparted to this hybrid material from the decoration of CdSe quantum dots on these narrow bandgap graphene nanoribbons derived from CNTs. Here we report such an unprecedented method of organization of CdSe QDs on graphene nanoribbons originating from the electrochemical oxidation of SWCNTs.

Scheme 1 describes the unzipping process followed by the organization of CdSe clusters on the instantaneously formed graphene nanoribbons. In a typical preparation, single walled carbon nanotubes (SWCNTs) were unzipped according to a recent procedure.⁸ The yield depends on the potential and time. For example, if the quality, thickness and homogeneity of the coating can be controlled, the yield could be about 70% after 15 hours. The potentials were selected on the basis of voltammograms of SWCNTs in 0.5 M H₂SO₄ (Fig. 1(a)) (the potential is marked by a violet arrow) where oxygen evolution just starts. During the last stage of reduction step facilitating the formation of graphene, CdSO₄ and Na₂SeO₃ were added in the mixture. Again the potential was chosen carefully so that simultaneous reduction of oxidized CNTs and co-deposition of CdSe particles could be achieved. Accordingly, Fig. 1(a) represents the cyclic voltammogram (CV) of the oxidized nanotubes in the presence of Cd and Se-precursors (red line). Two oxidation (A1, A2) and two reduction peaks (C1, C2) along with a small hump (A1′) were identified in the voltammogram at A1 = 0.09 V,

Physical and Materials Chemistry Division, National Chemical Laboratory, Pune-411008, India. E-mail: vk.pillai@ncl.res.in; Fax: +91 20 2590 2636; Tel: +91 20 2590 2566

† Electronic supplementary information (ESI) available: Experimental details and supporting figures. See DOI: 10.1039/c2cc17749h

‡ Present address: Central Electrochemical Research Institute, Karaikudi, Tamilnadu, 630006, India.

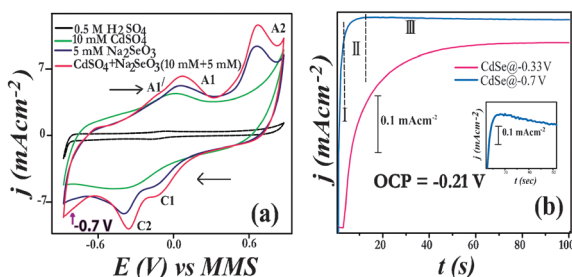


Fig. 1 (a) Cyclic voltammogram of unzipped SWCNTs during the reduction at -0.7 V and in the presence of 10 mM CdSO_4 , 5 mM Na_2SeO_3 and a mixture of both the species, (b) i - t transient during electrodeposition of CdSe at -0.33 and -0.7 V.

$A_2 = 0.7$ V, $A_1^1 = -0.16$ V and $C_1 = -0.09$ V, $C_2 = -0.38$ V vs. mercury-mercurous sulfate (MMS) respectively. In order to identify the corresponding peaks, cyclic voltammograms were recorded for graphene nanoribbons (GNRs) (unzipped SWCNTs) separately in 0.5 M H_2SO_4 , 10 mM CdSO_4 and 5 mM Na_2SeO_3 (black, green and blue lines respectively). The voltammogram obtained in CdSO_4 showed one redox couple (0.07 and -0.39 V vs. MMS) corresponding to Cd^{2+} reduction and oxidation respectively. The peaks A_1/C_1 constitute a couple for oxidized SWCNTs (un-SWCNTs) in 0.5 M H_2SO_4 and the peaks could be assigned to the quinol-hydroquinone couple on oxidized SWCNT walls.¹⁰ However, these peaks vanished when CV was carried out in a 10 mM CdSO_4 solution leaving the features due to predominant Cd^{2+} redox reaction (green curve).

The peaks observed in the case of Na_2SeO_3 are A_1^1 (H_2Se to Se), A_1 (H_2Se to Se), A_2 (Se to H_2SeO_3), C_1 (H_2SeO_3 to grey Se), and C_2 (grey Se to red Se through H_2Se formation). The assignment of all these peaks is in accordance with a previous study on the reduction of sodium selenite in H_2SO_4 .¹¹ Interestingly, the CV of oxidized SWCNTs in a mixture of CdSO_4 and Na_2SeO_3 follows similar feature as observed in the case of only Na_2SeO_3 . Indeed, H_2Se , formed during the electroreduction of selenite combines with Cd to form CdSe. CdSe nanoparticles so formed are anchored by the functional groups present on the unzipped SWCNT surfaces (formed during the oxidative unzipping process) (Section S5, ESI†).

In order to determine the suitable potential for reduction and to investigate the mechanism of deposition, chronoamperometry was performed at two different potentials (-0.33 V and -0.77 V vs. MMS respectively), which are more negative than the open circuit potential (OCP) of the system (0.58 V vs. MMS) for 100 s. Accordingly, Fig. 1(b) shows the chronoamperogram for the deposition. Both the plots show initial sharp increase in current density due to double layer charging effect and local currents. The current transient then steadily increases to show a shoulder (or hump) followed by a minor decrease to a certain value eventually reaching a plateau. The peak maximum, however, increases and becomes more pronounced as the deposition potential becomes more negative (-0.33 V to -0.7 V) as has been predicted by classical nucleation theory. The electrodeposition has been carried out at -0.7 V. In order to unravel the nucleation process, the current-time transient obtained at -0.7 V has been subdivided into 3 zones (Fig. 1(b))—I, II and III. Linearity of current density vs. $t^{1/2}$

for zone-I (*i.e.*, before peak maxima) is indicative of instantaneous nuclei formation with hemispherical growth. There are two models available to describe nucleation—instantaneous and progressive. A plot of two dimensionless numbers namely $(i/i_m)^2$ and t/t_m gives information about either of the above mechanisms. Fig. S2 (a,b) (ESI†) represents the fitting of experimental data with those obtained from equations (S1) and (S2) (ESI†, S2) (zone-II). Near the peak maximum in the reduced current-time curve, the deposition can be described well by equation (S1) and at this time CdSe deposition occurs instantaneously with hemispherical growth. However, during the short-time regime (zone-I) there is a strong competition between progressive and instantaneous nucleation although the instantaneous mechanism is more pronounced.

Fig. S3 (ESI†) shows the X-ray diffraction pattern of the unzipped SWCNT-CdSe composite (denoted un-SWCNT + CdSe) which confirms the formation of CdSe nanoparticles on unzipped nanotubes. The main diffraction peak is observed at 23° (broad) corresponding well to the (100) reflection of primitive hexagonal CdSe reported previously (JCPDS 77-0046).¹² Other broad peaks (at 36.5° , 42.8° , 49.4° and 56.3°) also match very well with the same crystal structure of CdSe. The (002) peak of SWCNT/graphitic structure is overlapped with the (100) peak of CdSe and hence is not clearly visible. In fact, the appearance of so many peaks proves the polycrystalline nature of CdSe particles and the broadening of the XRD peaks reveals that the particles are in the nanometre range.

In order to further confirm the unzipping of SWCNTs and subsequent deposition of CdSe on them under electrochemical conditions, we have carried out micro Raman study at various stages of the unzipping process concomitant to the CdSe anchoring. Accordingly, Fig. 2 describes the micro Raman spectra for (i) pristine SWCNTs before unzipping, (ii) SWCNTs upon subjecting to 0.8 V and (iii) GNRs after CdSe decoration at -0.7 V. The intensity ratio of the two phonon modes, namely D-band and G-band, is found to increase from 0.08 to 0.86 after subjecting the SWCNTs to 0.8 V for 10 h. This indicates the increase of defects after electrochemical oxidation. One of the more striking features of the Raman spectra is the disappearance of the so-called RBM band of pristine SWCNTs (258.1 cm^{-1} corresponding to metallic nanotubes) upon 6 h oxidation. This is in agreement with the previously observed report that metallic CNTs are more susceptible towards electronic attack than their semiconductor analogues.⁹ The intensity of other two RBM phonon modes (due to semiconducting nanotubes)

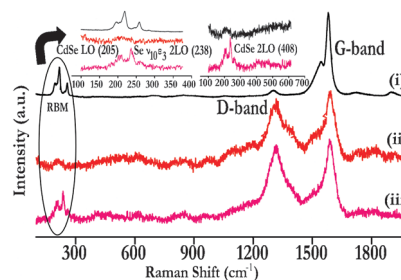


Fig. 2 Micro Raman spectra of (i) pristine SWCNTs (before unzipping), (ii) SWCNTs after unzipping at 0.8 V for 10 h and (iii) unzipped SWCNTs after CdSe decoration at -0.7 V. All the spectra are recorded using a 632.8 nm laser with 20 mW power.

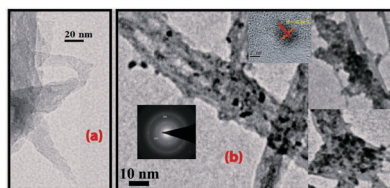


Fig. 3 Bright field low resolution TEM images of (a) only GNRs and (b) CdSe–GNR composite. Inset shows single CdSe nanoparticles and SAED pattern.

also gets strongly decreased, suggesting the opening of CNTs (unzipping) perhaps with concomitant formation of graphene nanoribbons. The application of external anodic potential modulates the Fermi level of CNTs and facilitates oxidative unzipping since anodic bias gives rise to defect sites which thereby disrupts the symmetry of electron distribution on CNTs, rendering the surrounding carbon atoms more reactive. This activation helps to propagate the defects along the tubular axis of CNTs and eventually opens up the nanotubes to form graphene. Addition of CdSO_4 and Na_2SeO_3 in the same solution during reduction is expected to generate CdSe nanoparticles which subsequently bind to the functional groups on the GNRs. Fig. 2(iii) shows the Raman spectrum of the GNRs after CdSe decoration. For example, the spectrum clearly indicates the presence of CdSe NPs since in the low frequency region ($200\text{--}300\text{ cm}^{-1}$ inset of Fig. 2(ii)), the peak corresponding to the LO phonon of CdSe NPs (205 cm^{-1}) is distinctly observed. More interestingly, the appearance of the LO phonon at 205 cm^{-1} as compared to that of bulk CdSe (210 cm^{-1}) suggests the formation of small clusters of CdSe on GNRs.¹² Moreover, a broad two photon 2LO band for CdSe NPs is also observed at 408 cm^{-1} . The peak at 238 cm^{-1} can be assigned to the ν_{10} (ϵ_3) mode of phonon vibration of selenium, confirming the presence of excess selenium during electrodeposition.

Low resolution TEM micrographs (Fig. 3(a) and (b)) show the formation of CdSe nanoparticles on unzipped SWCNTs. The average diameter of the SWCNTs varies from 1.1 to 2 nm (Fig. S9, ESI[†]). However, after the unzipping process, the diameter increases up to 5–6 nm (as theoretically expected), indicating the transformation of SWCNTs into graphene by longitudinal unzipping in the presence of the electric field although it is difficult to get a single large sheet of graphene from the unzipping of SWCNTs since only at selected positions such individual sheets are observed on the TEM grid. On the other hand, fully or partially unzipped tubes are entangled together and appear as 40–50 nm wide, bundled sheets in most places, depending also on the sample preparation procedures. These small particles then coalesce in the presence of excess precursor, with the time of deposition, eventually forming larger clusters, typically after 1 h (for example, 15–20 nm after 15 min and 40–50 nm after 1 h to cover the GNRs as shown in Fig. S9, ESI[†]). Selected area electron diffraction in the inset of Fig. 3 gives d -spacings, which is in fair agreement with the d -spacings of primitive hexagonal CdSe. Fig. 3 inset displays a high resolution TEM image of one individual CdSe quantum dot, where the d -spacing from the lattice fringes also matches well with that of the hexagonal CdSe. Finally Fig. S4 (ESI[†]) shows a representative EDAX spectrum of the as-prepared composite,

confirming the presence of CdSe in the composite corresponding to a Cd to Se ratio of $\sim 1 : 2$.

The disappearance of characteristic van Hove's singularities of p-SWCNTs between 400–800 nm and concomitant emergence of a new broad peak at around 576 nm after unzipping in the corresponding absorbance spectra (Fig. S5, ESI[†]) suggest the formation of graphene nanoribbons as well as the *in situ* formation of small CdSe quantum dots. Interestingly photo-conductivity measurement of this composite material shows an almost double increment in conductivity after irradiation with 1.5 AM light (Fig. S5, ESI[†]). Further, steady state (solid state) photoluminescence (PL) measurement of this composite material shows effective PL quenching (Fig. S3, ESI[†]), thereby implying that this material could be promising for solar cells and photocatalysis. PL quenching also suggests the proper contact between CdSe and GNRs, thereby paving the way for easy transfer of photogenerated electrons from CdSe to highly conducting GNRs.

In conclusion, we have developed an unprecedented method of generating CdSe Q-dots on graphene nanoribbons by an *in situ* electrochemical unzipping of SWCNTs followed by a second reduction step of the oxidatively unzipped SWCNTs. The method is simple, cost effective and gives better distribution of uniform CdSe decoration on graphene surface with accurate size control. We believe that these hybrid materials will have unique behavior such as optical and electrical properties for applications in quantum dot sensitized solar cells, photoelectrochemical water splitting cells, photocatalysis *etc.* because of direct linker-free heterojunction formation of CdSe and graphene nanoribbons compared to similar composites made through other routes. Further experiments are in progress to explore their applications for thin, lightweight, flexible optoelectronic devices.

Notes and references

- (a) K. S. Novoselov, Z. Jiang, Y. Zhang, S. V. Morozov, H. L. Stormer, U. Zeitler, J. C. Maan, G. S. Boebinger, P. Kim and A. K. Geim, *Science*, 2007, **315**, 1379; (b) C. N. R. Rao, A. K. Sood, R. Voggu and K. S. Subrahmanyam, *J. Phys. Chem. Lett.*, 2010, **1**, 572.
- K. S. Novoselov, A. K. Geim, S. V. Morozov, D. Jiang, M. I. Katsnelson, I. V. Grigorieva, S. V. Dubonos and A. A. Firsov, *Nature*, 2005, **438**, 197.
- A. P. Alivisatos, *Science*, 1996, **271**, 933.
- (a) S. Sun, L. Gao, Y. Liu and J. Sun, *Appl. Phys. Lett.*, 2011, **98**, 931121; (b) Y. Zhang, T. Mori, L. Niu and J. Ye, *Energy Environ. Sci.*, 2011, **4**, 4517.
- (a) X. Geng, L. Niu, Z. Xing, R. Song, G. Liu, M. Sun, G. Cheng, H. Zhong, Z. Liu, Z. Zhang, L. Sun, H. Xu and L. Liu, *Adv. Mater.*, 2010, **22**, 638; (b) I. Robel, B. A. Bunker and P. V. Kamat, *Adv. Mater.*, 2005, **17**, 2458.
- Y. T. Kim, H. J. Han, B. H. Hong and Y. U. Kwon, *Adv. Mater.*, 2010, **22**, 515.
- D. V. Kosynkin, A. L. Higginbotham, A. Sinitskii, J. R. Lomeda, A. Dimiev, B. K. Price and J. M. Tour, *Nature*, 2009, **458**, 872.
- D. B. Shinde, J. Debgupta, A. Kushwaha, M. Aslam and V. K. Pillai, *J. Am. Chem. Soc.*, 2011, **133**, 4168.
- C. A. Dyke and J. Tour, *J. Phys. Chem. A*, 2004, **108**, 11151.
- R. Kannan, U. Bipinlal, S. Kurungot and V. K. Pillai, *Phys. Chem. Chem. Phys.*, 2011, **13**, 10312.
- A. M. Espinosa, M. L. Tascon, M. D. Vazquez and P. S. Batanero, *Electrochim. Acta*, 1992, **37**, 1165.
- C. T. Giner, A. Debernardi, M. Cardona, E. M. Proupin and A. I. Ekimov, *Phys. Rev. B: Condens. Matter*, 1997, **57**, 4664.